# FULL-DISK OBSERVATIONS OF SOLAR OSCILLATIONS FROM THE GEOGRAPHIC SOUTH POLE: LATEST RESULTS*

*(Invited Review)*

GÉRARD GREC

*Department D'Astrophysique de l'I.M.S.P., E.R.A. du C.N.R.S.*
*Université de Nice, Parc Valrose F-06034, Nice Cedex, France*

ERIC FOSSAT

*Observatoire de Nice, BP252, 06007 Nice Cedex, France*

and

MARTIN A. POMERANTZ

*Bartol Research Foundation of The Franklin Institute, University of Delaware, Newark, Delaware, U.S.A.*

**Abstract.** This paper presents the latest results obtained from the analysis of the full-disk Doppler shift observations obtained at the geographic South Pole in 1981. About 80 normal modes of oscillation ($l$ = 0–3) have now been identified. Their frequencies range from 1886 μHz ($l$ = 1, $n$ = 12) to 5074.5 μHz ($l$ = 2, $n$ = 35), and their amplitudes are as low as 2.5 cm $s^{-1}$. Amplitude modulation occurs with periods of 1–2 days, and the individual oscillations appear to be excited randomly and independently. In cases where other groups have observed some of the modes identified by us, the agreement in frequency is good.

## 1. Introduction

The first uninterrupted observations of the Sun significantly longer than one day were made at the geographic South Pole during the first week of 1980. They consisted of Doppler shift measurement integrated over the entire solar disk, using a sodium cell optical resonance spectrometer (Grec *et al.*, 1976). The very high temporal resolution provided by the unusual duration (5 days) of this continuous data set has made it possible, for the first time, to resolve many individual normal modes of the oscillation of the solar sphere. A preliminary analysis of these data has already been published (Grec *et al.*, 1980). The present paper describes the more complete results which have since been obtained. They include the unambiguous identification of about 80 different normal modes. This identification has now made possible the use of the standard inversion technique for a seismological investigation of the solar internal structure (Christensen-Dalsgaard and Gough, 1981; Scuflaire *et al.*, 1982).

* Proceedings of the 66th IAU Colloquium: *Problems in Solar and Stellar Oscillations*, held at the Crimean Astrophysical Observatory, U.S.S.R., 1–5 September, 1981.

*Solar Physics* **82** (1983) 55–66. 0038–0938/83/0821–0055$01.80.

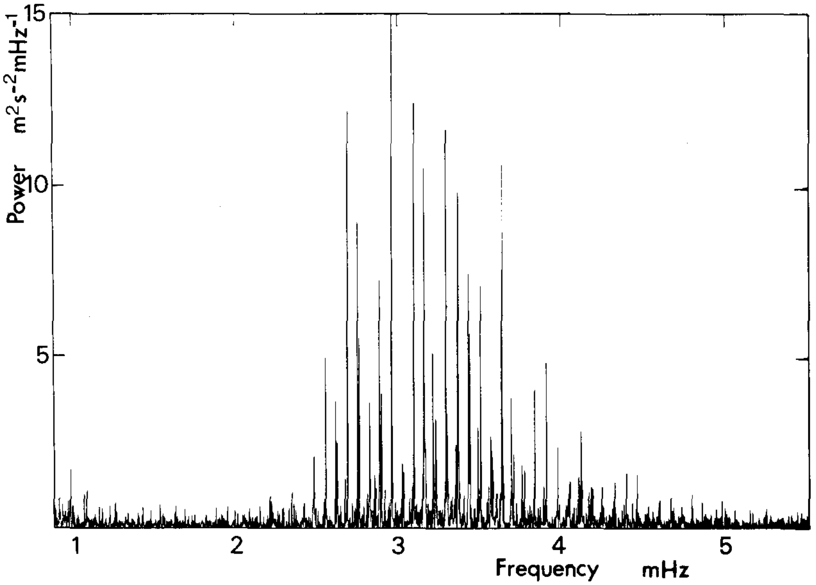


Fig. 1. Power spectrum of the South Pole data, which consists of the full-disk Doppler shift measurements recorded during the first week of January, 1980. The sample analyzed here has a duration of about 6 days, including three gaps of 2 to 3 hr. The frequency resolution is $\Delta\nu = 1.97$ μHz.

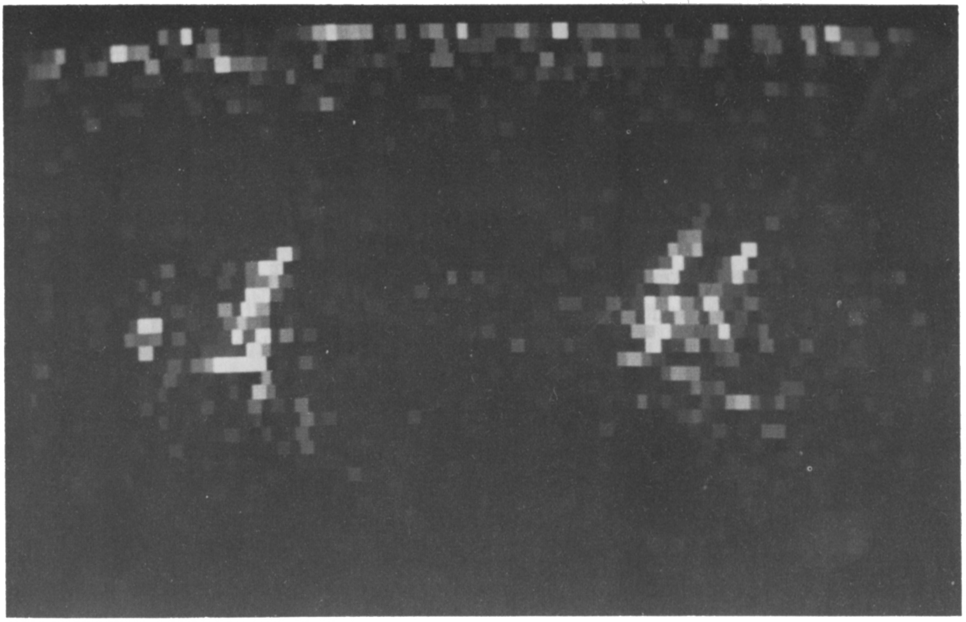

Fig. 2. Same as Figure 1, but the spectrum is now cut into slices of 136 μHz each. Each slice is displayed under the previous one on a video screen. The two lines on the right are the modes of even degrees ($l = 0$ is at the extreme right). The curvature of the four lines displays the departure from equidistance of the four sequence of radial harmonics. This curvature, which is expected from theory, even in the asymptotic approximation, makes possible the identification of each peak with its radial order, leaving room for almost no ambiguity. The first line displayed at the top of the picture starts at the frequency $\nu = 295.7$ μHz.

https://doi.org/10.1017/S0252921100095397 Published online by Cambridge University Press

TABLE I

List of frequencies (in μHz) of normal modes which have been identified in the South Pole data

| $n$ \ $l$ | 0 | 1 | 2 | 3 |
|---|---|---|---|---|
| 12 | | 1886.5 | 1947.5 | |
| 13 | 1958.5 | 2021 | | |
| 14 | 2093 | 2157 | 2217 | |
| 15 | 2229 | 2294 | 2352 | |
| 16 | 2363 | 2427.5 | 2486 | |
| 17 | | 2560.5 | 2621.5 | 2679 |
| 18 | 2631 | 2694 | 2756 | 2813 |
| 19 | 2765.5 | 2829.5 | 2890 | 2948.5 |
| 20 | 2900.5 | 2964.5 | 3026.5 | 3087 |
| 21 | 3034 | 3099 | 3161 | 3219.5 |
| 22 | 3169.5 | 3234 | 3296 | 3353.5 |
| 23 | 3303.5 | 3370 | 3432 | 3490 |
| 24 | 3442 | 3506.5 | 3568 | 3628.5 |
| 25 | 3578 | 3640.5 | 3701 | 3765.5 |
| 26 | 3714.5 | 3779.5 | | 3900 |
| 27 | | 3915.5 | | 4035.5 |
| 28 | | 4051.5 | 4111 | 4173 |
| 29 | 4123 | 4193 | 4252 | |
| 30 | 4262 | 4327 | 4389 | 4446 |
| 31 | 4399.5 | 4464 | 4526 | 4583.5 |
| 32 | 4537 | 4603 | 4663 | |
| 33 | 4673 | 4742 | 4800 | |
| 34 | | | 4937 | |
| 35 | | | 5074.5 | |

N.B.: 1 – The authors apologize for the fact that this list is not identical to the one which had been distributed during the meeting. A scaling error was hidden in the program of analysis and resulted in a decrease of all frequencies by a factor 0.9989.

We also call attention to a typographical error in the caption to Figure 1 in the preliminary power spectrum published in Grec *et al.* (1980). That figure actually comprised data extending over only 3.5 days, in contrast with Figure 1 in the present paper.

However, the other figures in the earlier paper did, in fact, cover the continuous 5-day run.

N.B.: 2 – Two pairs of even modes have not been listed because, as can be seen in Figures 2 and 3, the power spectrum displays for both these pairs a unique peak located in between the interpolated frequencies of $l = 0$ and $l = 2$ modes.

## 2. Radial Order Identification

In Grec *et al.* (1980), a superposed frequency analysis assuming a uniform spacing of 136 μHz was used to identify the degree $l$ of each individual peak. However, this procedure did not allow the identification of the radial order $n$ because the lowest order modes have too small amplitudes to be measured. This ambiguity, in fact, can be resolved thanks to the fact that the spectral peaks are not uniformly spaced. This is illustrated by Figure 2 which shows the same power spectrum as that in Figure 1, uniformly cut into slices of 136 μHz, with each slice displayed below the previous one.

https://doi.org/10.1017/S0252921100095397 Published online by Cambridge University Press

In such a display, a uniform frequency spacing between consecutive radial harmonics would provide a distribution of power along straight lines (vertical for a spacing of 136 μHz). The curvature observed is then indicative of the departure from this uniform spacing. This general behaviour can be compared with an asymptotic approximation given by Tassoul (1980):

$$\nu(n, l) = \nu_0\left(n + \frac{l}{2} + \varepsilon\right) + [l(l+1) + \delta]\frac{A\nu_0^2}{\nu}$$

in which $\nu$ is the frequency,

$$\nu_0 = \left[2\int_0^R \left(\frac{\mathrm{d}r}{c}\right)\right]^{-1}, \qquad c = \text{sound speed}\,,$$

$$\varepsilon = \frac{n_e}{2} + \frac{1}{4}\,,$$

and $A$, $\delta$, and $n_e$ are constant integrals of the solar model.

This comparison has been made by Grec (1981) who found values of $A \approx 0.267$ and $\delta \approx -17$. Being given those two numbers, the value of $\varepsilon$ depends on the identification of the order $n$ of the modes. Keeping in mind that $n_e$ has something to do with a polytropic index in Tassoul's calculation, the most reasonable values of $n$ must provide a value of $\varepsilon$ of the order of 1. This leads to a possible identification of the order $n$ of each observed normal mode, as summarized in Table I. The frequencies listed in this table have been estimated through the barycentre of each peak, which is in certain cases very broad (10 μHz or more), as illustrated by the mode ($l = 1$, $n = 25$, $\nu = 3.64$ mHz). There are a few pairs of even modes which cannot be separated and, consequently, have not been listed although they are located in a frequency range which contains considerable power.

The same identification has been made independently by Christensen-Dalsgaard and Gough (1981), using no asymptotic approximation, but only least square differences between oscillation frequencies calculated with an almost standard solar model and our observed frequencies.

## 3. Amplitudes

As we will see in the next section, the amplitude of each individual oscillation is randomly modulated with a characteristic time of about two days. Consequently the use of a sample of data the duration of which is about 6 days does not allow to measure each amplitude with an uncertainty lower than about a factor two. This fact must be kept in mind when using the numbers listed in Table II. These amplitudes have been calculated by integrating the power in a bandwidth of 4 to 8 μHz around each peak frequency and by substracting the mean background noise. The amplitude is not listed if the signal to noise ratio was not larger than 2, in power.

## 4. Lifetime of Oscillations

Figure 2 clearly shows that the mean width of the peaks is broader than the intrinsic resolution of the data set, which is equal to 1.97 μHz. To estimate the average shape of these peaks, a superposed frequency analysis has been carried out in a more precise way than that originaly used by Grec *et al.* (1980). For this purpose, the curvature of the 'vertical' lines in Figure 2 has been estimated by fitting a polynomial as an additive component to $\Delta\nu$ = constant. The best choice of this polynomial was found to be:

$$\Delta\nu = 134.40 + 0.011\,(n_0 - 13.5)^2\,,$$

where $n_0$ represents the line taken as the order of the radial (l = 0) normal mode frequency present in this line. $\Delta\nu$ is the spacing between line $n_0$ and line $(n_0 + 1)$. As is shown in Figure 3, the sliced spectrum now displays power lines which are roughly vertical and can be used for vertical additions.

A vertical sum covering the entire frequency range which contains significant power (from line 10 to line 35) is shown in Figure 4. The following numbers measured on this

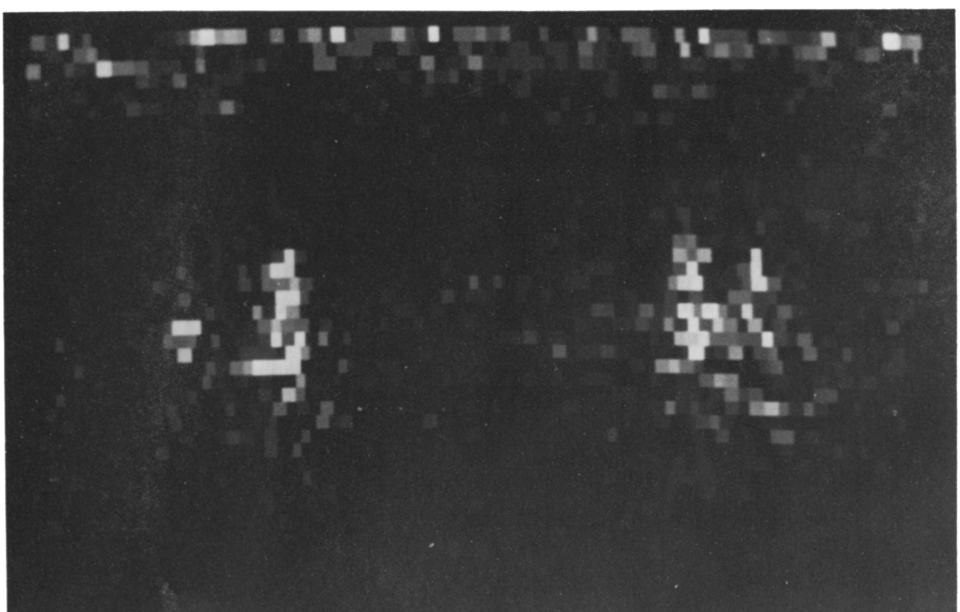

Fig. 3. Same as Figure 2, but each slice of the spectrum has been translated to make the power appear to be distributed in vertical lines. This was accomplished by replacing the constant spacing $\Delta\nu$ = 136 μHz by the polynomial $\Delta\nu = 134.40 + 0.011\,(n_0 - 13.5)^2$ (see text for details).

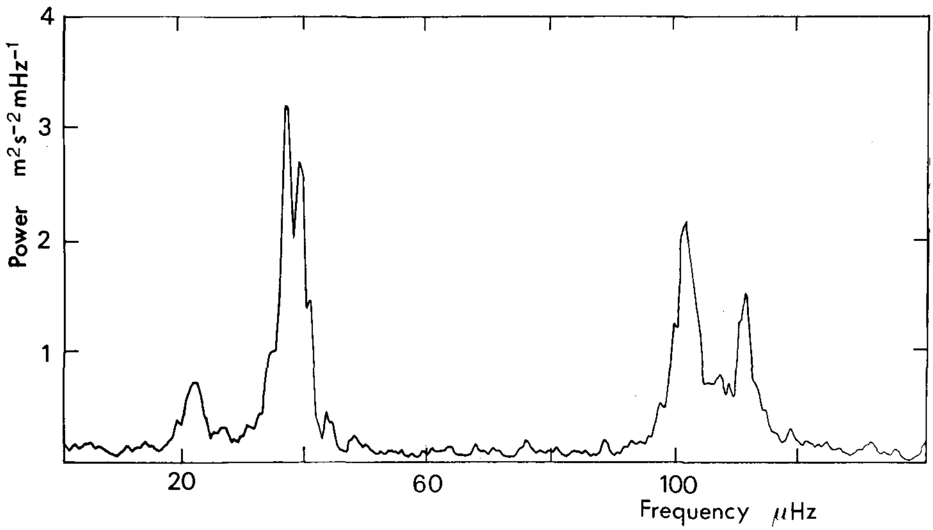


Fig. 4. A vertical summation of Figure 3 (superposed frequency analysis following the curvature) shows the mean shape of the four spectral peaks corresponding to normal modes of degree 3, 1, 2, and 0 (left to right).

figure are of interest (weighted mean values over the whole frequency range):

$$\nu(0, n) - \nu(2, n-1) = 9.4 \ \mu\text{Hz}\,,$$

$$\nu(1, n) - \nu(3, n-1) = 15.3 \ \mu\text{Hz}\,,$$

$$\nu(0, n) - \nu(1, n-1) = 71.4 \ \mu\text{Hz}\,.$$

The mean shape of all four peaks is reasonably well fitted by an exponential function $e^{-|\nu - \nu_0|/\sigma}$ with $\sigma = 2.35$ μHz. However, it must be noted that this function is not indicative of the shape of any individual peak, because it is an average of many peaks which have different heights and different widths. A very important point is that the natural width appears to increase very rapidly with the frequency as is demonstrated by the next two figures.

In Figure 5, the sum comprises lines 10 to 20 (roughly, frequencies below 3 mHz). In this case, the shape appears to be consistent with almost monochromatic peaks broadened only by the resolution of the analysis.

In Figure 6, the sum is made over the highest frequency range (above 3 mHz) and clearly proves that the peaks are much broader in this range. This tendency can be seen already on the power spectrum of Figure 1. It is also clearly seen on the power spectrum of brightness oscillations observed by the SMM spacecraft and analyzed by Woodard and Hudson (1983). This is not due only to a random scatter of the centroids of the individual resolved peaks, which could all be intrinsically sharp. There are several intrinsically broad peaks (e.g. $\nu = 3640$ and $\nu = 3432$ which have a width of respectively 9 and 7 μHz). There are also multiple peaks (such as $\nu = 3370$ or $\nu = 3578$) which have

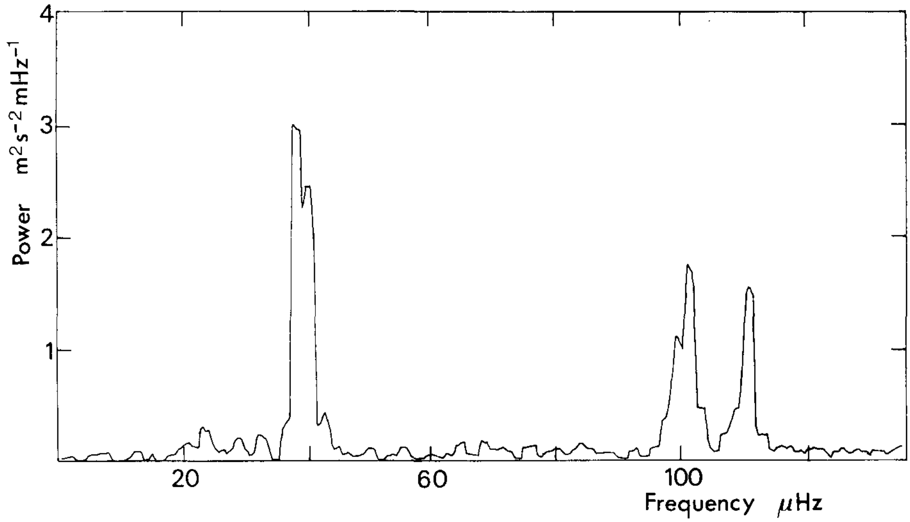


Fig. 5. Same as Figure 4, for frequencies below 3 mHz. The width of the mode $l = 0$ in this case is consistent with the resolution (1.97 μHz) of the data set. The slightly broader shape of the two others is not inconsistent with a small, unresolved, rotational splitting of about 0.5 μHz or less (although a small difference between the curvature of the four lines in Figure 2 can also result in a small difference among the widths of these three peaks).

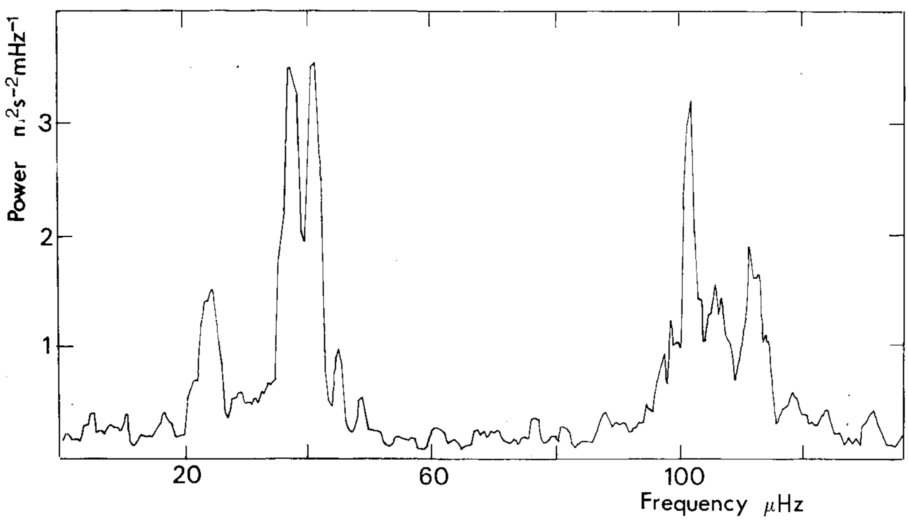


Fig. 6. Same as Figure 4, for frequencies higher than 3 mHz. It appears that the width of the spectral peaks increases dramatically in this frequency range.

to be regarded as a random distribution of power inside a broad envelope, which would be filled if the amount of data available was infinite.

These peaks are broadened, more and more with increasing frequency, by a modulation which can affect the amplitude, the frequency, or both. A direct information concerning the amplitude modulation has been obtained by cutting the data in 12 hr samples, and

TABLE II

List of amplitudes, in cm $s^{-1}$, of the normal modes identified in Table I. For the two pairs of even modes which cannot be separated in the power spectrum, the amplitude has been arbitrarily equidistributed (number in parenthesis).

| $n$ \ $l$ | 0 | 1 | 2 | 3 |
|---|---|---|---|---|
| 12 | | 2.5 | 3 | |
| 13 | 3.5 | 3 | | |
| 14 | 3.5 | 4 | 5 | |
| 15 | 4 | 3 | 4 | |
| 16 | 4 | 5 | 9 | 4 |
| 17 | | 11.5 | 11.5 | 6.5 |
| 18 | 9 | 21 | 14 | 6.5 |
| 19 | 11.5 | 13 | 15 | 7 |
| 20 | 12 | 22 | 7.5 | 6.5 |
| 21 | 7.5 | 17.5 | 21 | 14 |
| 22 | 10.5 | 13.5 | 20 | 11 |
| 23 | 10 | 23 | 15.5 | 7.5 |
| 24 | 14 | 15.5 | 13 | 6.5 |
| 25 | 9.5 | 24.5 | 12 | 7.5 |
| 26 | 9.5 | 8.5 | (9) | 6 |
| 27 | (9) | 11 | (10) | 6.5 |
| 28 | (10) | 8.5 | 10 | 6 |
| 29 | 12.5 | 9.5 | 8.5 | |
| 30 | 6 | 9.5 | 6 | 6 |
| 31 | 8 | 8.5 | 4 | 6 |
| 32 | 6 | 5.5 | 4 | |
| 33 | 6 | | 4.5 | |
| 34 | | | 4 | |
| 35 | | | 3.5 | |

by doing a Fourier analysis of each. In this case the resolution is not sharp enough to separate $l = 0$ from $l = 2$ or $l = 1$ from $l = 3$, but the odd and even pairs are separated. Figure 7 shows the power of the main pairs plotted as a function of time. For even pairs, the mixing between amplitude modulation and beating phenomena confuses the analysis. However, for odd pairs of peaks, the power is dominated by the contribution of $l = 1$ (except for 3.22 mHz), and the beating is almost negligible. Hence, it is essentially the amplitude modulation of the $l = 1$ modes which shows exponential increases or decreases with a typical time scale of the order or 1–2 days. Furthermore, there is no correlation between two neighboring harmonics.

Is there equipartition of a constant total power among all different normal modes, or is each mode independently and randomly excited and damped? Some information on this topic can be obtained from the time variation of the total power in the five-minute range (Figure 8). The r.m.s. relative fluctuation of the total power with time is 20%. Regarding the fact that there are essentially 30 main peaks which contribute to the total power, this r.m.s. fluctuation should have a value of about $(\sqrt{30})^{-1} \approx 18\%$ if each peak has an independant modulation of 100% in amplitude. This is in quite good agreement

https://doi.org/10.1017/S0252921100095397 Published online by Cambridge University Press

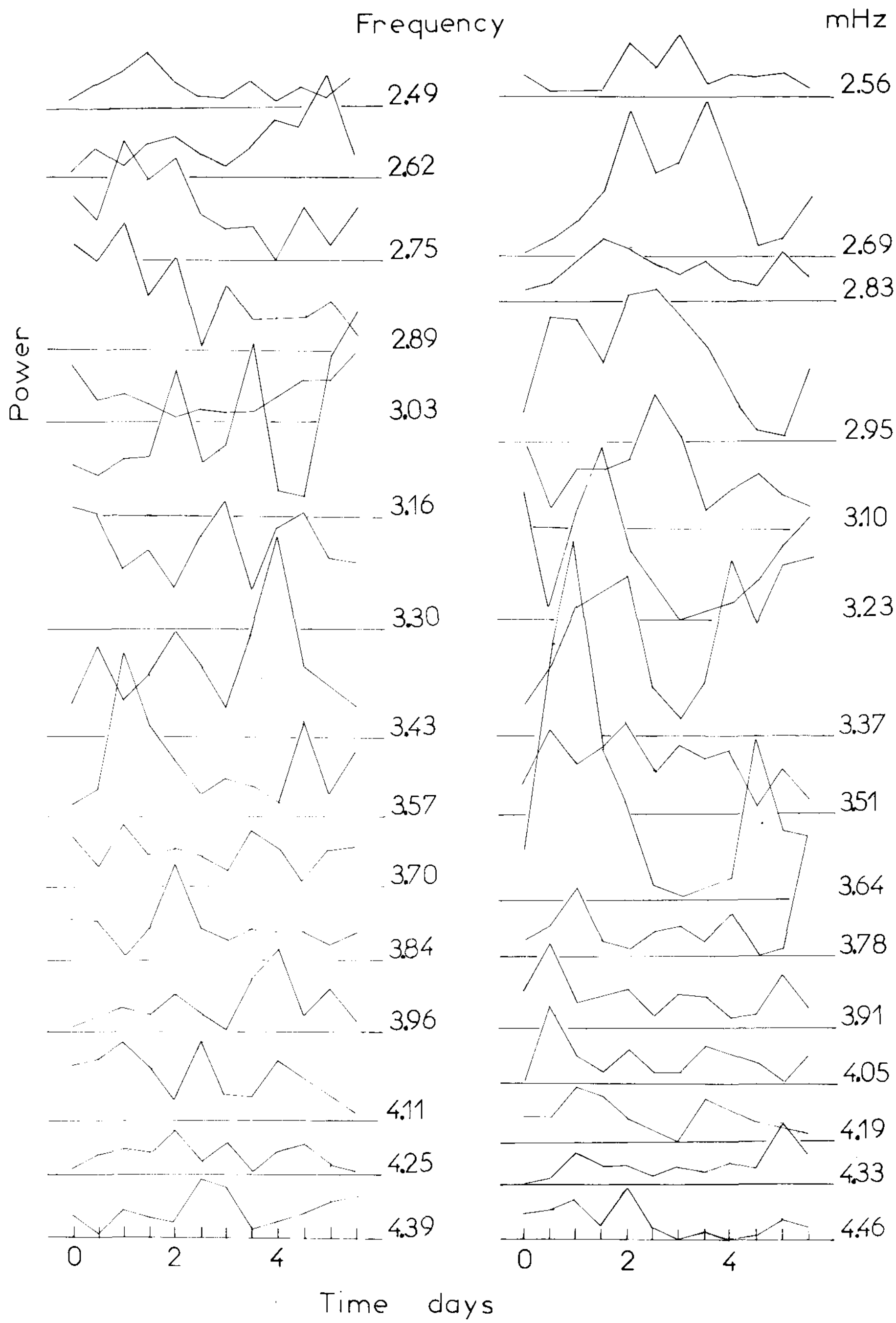


Fig. 7. Power, in $m^2 s^{-2}$, in each pair of even (left) or odd (right) peaks, versus time. The time series has been cut into samples of 12-hr durations for this analysis. The resolution in this case is 23 μHz, sharp enough to separate odd from even pairs, but not sufficient to resolve each individual mode inside a pair.

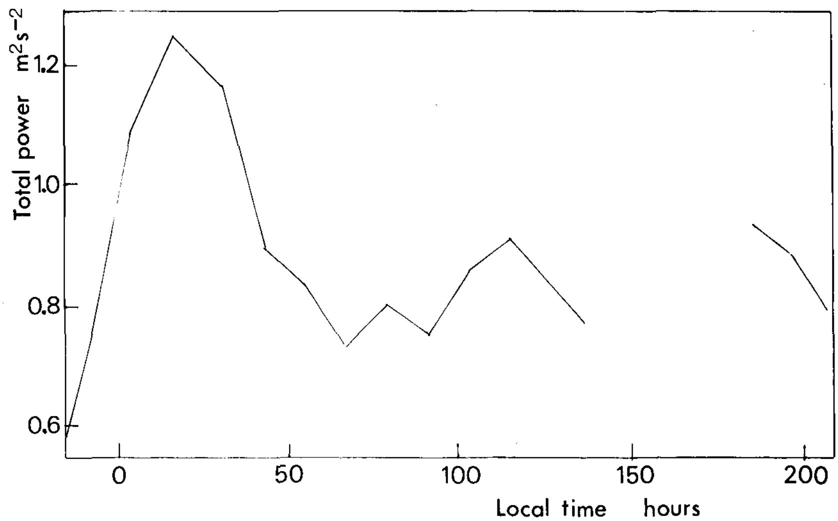


Fig. 8. Total power in the five-minute range (from 2 to 5 mHz) versus time. More data have been utilized in this figure than for the power spectrum, which was limited to the analysis of the almost continuous 6-day run.

with the measured value, and hence favors a random and independant excitation of each individual oscillation.

## 5. Discussion – Conclusions

(a) *Frequencies* – Table I contains many more frequencies than have been identified by any experiment conducted thus far. Where there is overlap, a comparison can be made with measurements by Claverie *et al.* (1981), Scherrer *et al.* (1983) and by Woodard and Hudson (1983). This comparison is shown in Figure 9, which displays all reported frequencies in a frequency-radial order coordinates diagram similar to Figure 2. The general agreement is quite satisfactory, since the mean difference between two observations never exceeds about 1 μHz. The scatter around the hypothetical continuous line which was fitted by a polynomial is also of the same order for all the different results, and this confirms the conclusion that the natural width of the peaks is a few μHz.

(b) *Lifetime* – An interesting question is to know if the oscillations are only amplitude modulated or also phase or frequency modulated. The characteristic time of the random modulation of amplitude displayed on the Figure 7 does not seem to change significantly with the frequency. Now it happens that the width of the spectral peaks does change by a very significant amount, with frequency. It may well be that the longest period oscillations maintain a long term phase coherence and are only modulated in amplitude. In this case, all the oscillations would have the same kind of amplitude modulation, while the lifetime of the phase would decrease dramatically at frequencies higher than 3 mHz. Further analysis and more data are required to clarify this issue.

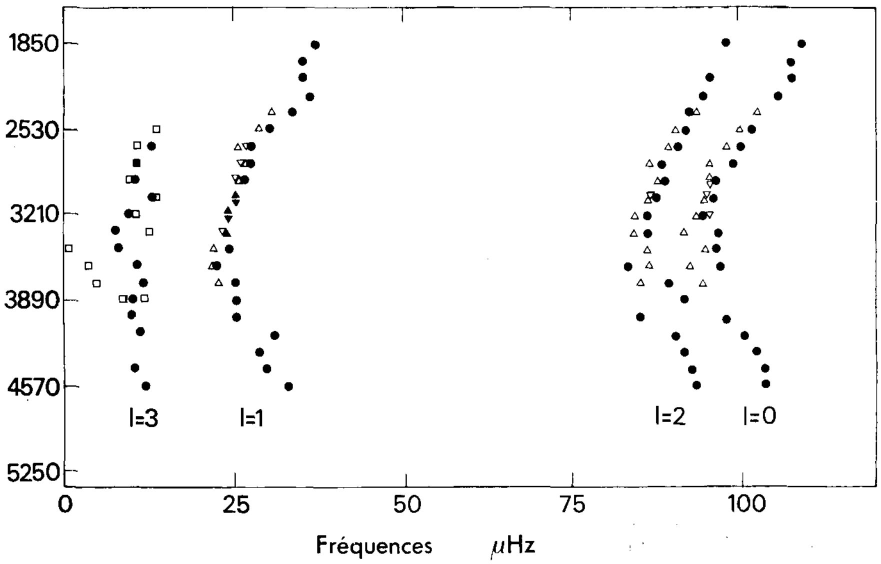


Fig. 9. Comparison of our frequencies determined from the South Pole data (●) with those published by Claverie *et al.* (△), Scherrer *et al.* (□), and Woodard and Hudson (▽). ▲, ■, and ▼ indicate coincidence (better than 0.5 μHz) with our frequencies.

(c) *Rotational splitting* – For frequencies smaller than 3 mHz, Figure 5 shows a peak width almost consistent with the resolution of the analysis in the case $l = 0$. In the case $l = 2$, we must keep in mind that the width contains the resolution of the observation (2 μHz), the unresolved splitting, the residual width of each split component and a possible slight extra-broadening due to the imperfect fitting of the real central frequencies with our polynomial. In these conditions, if the $l = 2$ modes are split in 5 components (or 3 if only the even values of $m$ can be seen), the relatively sharp mean peak on this Figure 5 (about 3.5 μHz) does not seem to be consistent with the relatively large frequency splitting (0.75 μHz) reported by Claverie *et al.* (1981). It may be that all split components have not equally contributed to the mean peak of Figure 5 because of the random amplitude modulation. It may also be that the reported 0.75 μHz splitting is an artifact of analysis. A basic difference between the two respective analysis is that we have made the superposition of Figures 4–6 by vertical summation of lines in Figure 3, while Claverie *et al.* have shifted each line to follow the apparent central component of the $l = 0$ peak. This procedure makes the shape of the $l = 2$ mean peak arbitrarily dependent upon the scatter of the $l = 0$ measured frequencies around their unknown real values (see Figure 9). Following the same procedure but normalizing on the central component of the $l = 2$ peak would make the average shape of $l = 2$ appear as a unique peak, and would split the $l = 0$ mean peak into a few components, separated by about the same amount (close to the resolution of their data). This is contrary to the fact that the $l = 0$ peak is non-degenerate.

This question of the splitting is a very important one which has not yet been satisfactorily answered. A display of the power spectrum on a figure similar to our

Figure 2 or 3 could probably help to avoid a possible confusion between real splitting and random distribution of power in a broad envelope.

(d) *Amplitudes* – Another interesting point to be mentioned is the sharp drop of amplitude with decreasing frequencies around 2.5 mHz. This drop (a factor 4 in power) appears to be limited to a narrow band close to 2.5 mHz, and for lower frequencies, the amplitude decreases slowly to reach the increasing noise level at about 1.9 mHz. This behavior will have to be explained by an adequate excitation – damping mechanism. Is there some coupling between *p*-modes and surface *g*-modes (2.5 mHz is not far from the buoyancy frequency of the solar atmosphere, above which no gravity mode can exist)? In any case, in the absence of any accurate prediction of the amplitudes of low-order, low-degree *p*-modes, the very slow decrease of amplitude can be regarded as very encouraging for the future progress of helioseismology. The next major step will hopefully be the detection of low-degree, low-order *p*-modes and a few *g*-modes. This detection may require only a moderate improvement of the sensitivity.

## Acknowledgements

This research is supported by the National Science Foundation's Division of Polar Programs under grant DPP 7822467.

## References

Christensen-Dalsgaard, J. and Gough, D. O.: 1981, *Astron. Astrophys.* **104**, 173.
Claverie, A., Isaak, G. R., McLeod, C. P., Van Der Raay, H. B., and Roca Cortes, T.: 1981, *Nature* **293**, 443.
Grec, G.: 1981, These de Doctorat, Universite de Nice.
Grec, G., Fossat, E., and Vernin, J.: 1976, *Astron. Astrophys.* **50**, 221.
Grec, G., Fossat, E., and Pomerantz, M.: 1980, *Nature* **288**, 541.
Scherrer, P., Wilcox, J., Christensen-Dalsgaard, J., and Gough, D. O.: 1983, *Solar Phys.* **82**, 75 (this volume).
Scuflaire, R., Gabriel, M., Noels, A., Grec, G., and Fossat, E.: 1982, preprint.
Woodard, M. and Hudson, J.: 1983, *Solar Phys.* **82**, 67 (this volume).